THE FORMATION OF CRATER CLUSTERS ON MARS BY ATMOSPHERIC DISRUPTION OF METEOROIDS

G. S. Collins[1], E. L. Newland[1], D. Schwarz[1], M. Coleman[1], S. McMullan[1], I. J. Daubar[2], K. Miljković[3], T. Neidhart[3] and E. K. Sansom[3]. [1]Department of Earth Science and Engineering, Imperial College, London, SW7 2AZ, United Kingdom (E-mail: g.collins@imperial.ac.uk); [2]Brown University, Providence, RI, USA; [3]Curtin University, Australia.

Introduction: Small impact features on Mars are regularly detected in images taken by orbiting spacecraft. More than half of these features are clusters of craters formed by the break-up of the meteoroid in Mars' atmosphere. A catalog of ∼1000 recent impacts [1] and detailed characterization of the crater clusters [2, 3] provide valuable observational constraints with which to calibrate models of atmospheric disruption of meteoroids on Mars. The calibrated model provides insight into the impactor flux at the top of Mars' atmosphere as well as the impact parameters at the ground, which is beneficial for efforts to detect and interpret seismic wave signals generated by cluster-forming impacts [4].

Here we model meteoroid fragmentation in the martian atmosphere using an implementation of the Separate Fragments Model [5, 6]. Crater sizes are predicted using π-group crater scaling relationships [7]. A Monte Carlo approach is used to generate a synthetic catalog of single-crater and crater-cluster forming impacts for comparison with observational data [8]. The spatial distributions, number and sizes of craters in recently mapped clusters provide valuable constraints on the properties of the impacting meteoroid population as well as key model parameters, including the lift coefficient and fragment separation velocity.

Martian Crater Clusters: The observational data used for model calibration comes from a catalog of ∼1000 recently formed single craters and crater clusters [1], the latter of which have been mapped and characterized in detail [2, 3]. The data set includes crater size and position information for all individual craters larger than one meter in detected clusters and single craters. From the cluster data, a number of cluster properties were derived that characterize the spatial distribution and size-frequency distribution of craters within the cluster [2, 3], including the number of craters and the effective diameter ($D_{\rm eff} = \sqrt[3]{\sum_i D_i^3}$, where D_i are the individual diameters of craters in the cluster [9]).

Cluster modelling: To model the formation of the observed single craters and crater clusters on Mars we used an implementation of the Separated Fragments Model [5, 6] (SFM). Meteoroid fragmentation is assumed to occur when the ram pressure on the meteoroid exceeds its internal strength ($\rho_a v^2 > \sigma_0$). When the initial strength of the meteoroid is exceeded, it is assumed to separate into two child fragments with a random mass ratio and azimuth, a lateral separation velocity proportional to the meteoroid speed, and with strengths σ_i that on average increase owing to their smaller mass and a Weibull law, but are subject to significant random variation. The child fragments are able to undergo further fragmentation, when $\rho_a v^2 > \sigma_i$, resulting in two new fragments and an additional separation velocity and so on. The products of fragmentation are tracked until they are totally ablated or impact the surface. On impact, the lateral position of each crater is recorded and crater size is calculated using strength-regime crater scaling relationships appropriate for weak, porous solids on Mars [7].

To produce a set of synthetic crater clusters for comparison with those observed on the surface of Mars, a number of Monte Carlo simulations were carried out. All simulations used the same drag coefficient and atmospheric density profile and began with the meteoroid at an altitude of 100 km. All other initial properties of the meteoroid were selected at random or according to parameter probability distributions for Mars. The probability distribution for pre-entry velocity was derived from [10] and for impact angle we assumed $P(>\theta) = \sin^2\theta$ [11]. Meteoroid mass was drawn from a distribution based on observations of terrestrial fireballs for meteoroids $>$ 3 kg [12]. Uniform probability distributions were used for meteoroid density and ablation parameter. As the distribution of meteoroid strength is of critical importance for the frequency of cluster formation and the characteristics of clusters, we adopt a log-uniform probability distribution and treat the bounds of this distribution among the principal unknowns in our analysis.

Results: Several Monte Carlo simulations were performed using the SFM to establish best-fit model parameters and meteoroid property distributions. The best-fit synthetic dataset of clusters and craters is remarkably consistent with the observed characteristics of martian crater clusters for effective diameters larger than 10 m (Fig. 1).

The model distribution of dynamic meteoroid strength that produces the best match to observations has a minimum strength of ∼50 kPa, a maximum strength of ∼5 MPa and a median strength of ∼0.3 MPa. An important feature of the model is that individual fragmentation events are able to produce fragments with a wide range of dynamic strengths as much as ten times stronger or weaker than the parent fragment.

Calibration of the model also constrains the separation

speed of fragments after break-up and the lift coefficient. The observed distribution of cluster aspect ratios is well reproduced with a lift coefficient $\sim 10^{-2}$, several times higher than previous estimates [5]. Similarly, to fit the observed median separation distance between crater pairs requires fragment separation speeds of $\sim$0.25% of the pre-entry meteoroid velocity, consistent with typical separation velocities inferred from terrestrial meteorite falls.

Discussion: The calibrated model can be used to estimate the current small meteoroid flux at Mars, for comparison with the terrestrial and lunar fluxes. For a Mars-Earth impact flux ratio of 1.3–2 (at the top of the atmosphere), the calibrated model implies a rate of small impacts ($D_{\text{eff}} > 10$ m) on Mars 1.5–4 times higher than recent observation-based estimates [13]. This suggests that many meter-to-decameter craters forming on Mars are not detected with current orbital imaging. Alternative methods of detecting small impacts on Mars, such as by the seismic signals that they generate, would be of immense value.

The model results also provide insight into properties of the meteoroids that produce single craters and clusters. The formation of crater clusters is favored by low-to-moderate impact speeds, low meteoroid strengths and relatively steep trajectories to the surface. Conversely, single crater formation is favored by relatively shallow trajectories and high strengths.

The success of the Separate Fragments Model in reproducing the diversity of observed clusters suggests that future efforts to infer impactor properties from observed cluster characteristics by inversion may be fruitful. This would allow impactor properties relevant to seismic wave generation, such as the total impact momentum, major fragmentation altitudes and the times between fragment impacts, to be inferred from cluster characteristics.

Acknowledgments: GSC was funded by UK Space Agency grant ST/T002026/1. IJD was funded by NASA award 80NSSC20K0789. TN, KM and EKS were funded by the Australian Research Council (DE180100584, DP180100661 and DP200102073).

References: [1] Daubar, I. J. et al. (2022) *JGR-Planets*, submitted. [2] Daubar, I. J. et al. (2019) *JGR-Planets*, 124:958–969. [3] Neidhart, T. et al. (2022) *JGR-Planets*, submitted. [4] Schmerr, N. C. et al. (2019) *JGR-Planets*, 124. [5] Passey, Q. R. & Melosh, H. J. (1980) *Icarus*, 42:211–233. [6] Artemieva, N. A. & Shuvalov, V. V. (2001) *JGR-Planets*, 106:3297–3309. [7] Holsapple, K. A. (1993) *Ann. Rev. Earth Planet. Sci.* 21:333–373. [8] Collins, G. S. et al. (2022) *JGR-Planets*, submitted. [9] Malin, M. C. et al. (2006) *Science*, 314:1573–1577. [10] Le Feuvre, M. & Wieczorek, M. A. (2011) *Icarus*, 214:1–20. [11] Shoemaker, E. M. (1961) *Physics and Astronomy of the Moon* ed. by Z. Kopal Academic Press, 283–359. [12] Bland, P. A. & Artemieva, N. A. (2006) *MAPS*, 41:607–631. [13] Daubar, I. J. et al. (2013) *Icarus*, 225:506–516.

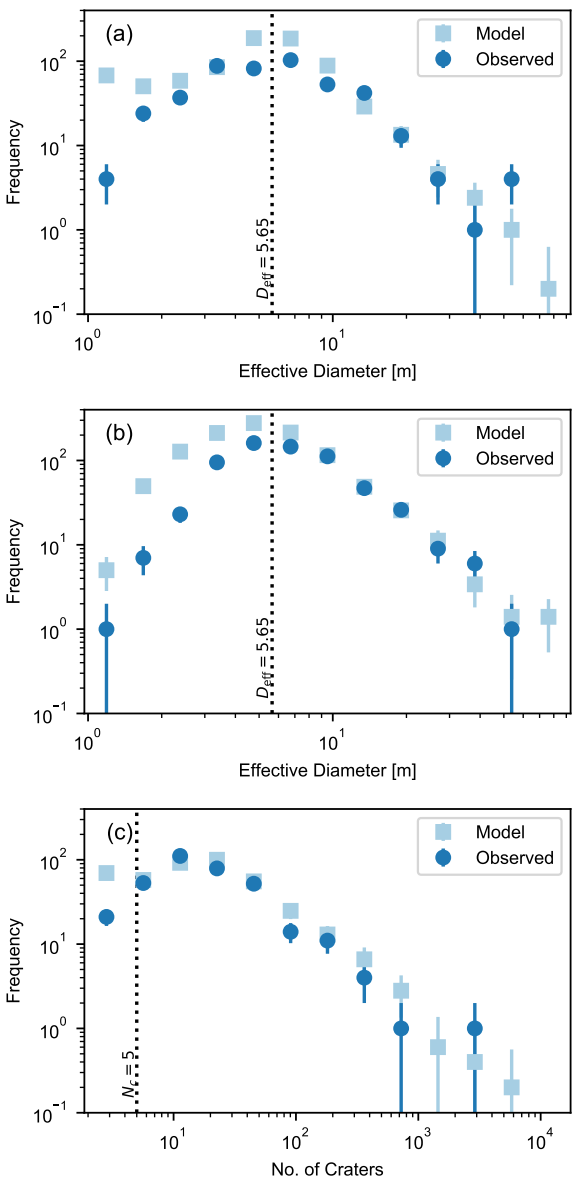

Figure 1: Incremental relative frequency distributions of (a) diameter of singular craters; (b) effective diameter of crater clusters; (c) number of craters in a cluster predicted by the best-fit model compared with observations. Error bars for the models and observations are $\sqrt{N}$. The dotted lines indicate the threshold effective diameter (a), (b) and number of craters in the cluster (c) above which the model was calibrated to observations.